*Iraqi Journal of Physics, 2024* *Vol. 22, No. 1, PP.75-81*

*https://doi.org/10.30723/ijp.v22i1.1197* *P-ISSN: 2070-4003*
*E-ISSN: 2664-5548*

# Optical Investigation of Reduced Graphene Oxide / Titanium Dioxide Nanocomposite Thin Films Synthesized by Hydrothermal Method

**Linda I. Mohi[1a], Ameer F. Abdulameer[1b*]**
[1]*Department of Physics, College of Science, University of Baghdad, Baghdad, Iraq*
[a]E-mail: *linda.ismail1604a @ sc.uobagdad.edu.iq*
[b*]Corresponding author: *ameer.abdulameer@sc.uobaghdad.edu.iq*

## Abstract

The growing need for unique optical properties in the manufacturing of electronic devices has led the world to the field of hybrid materials and their composites. In this study, a simple physical technique was used to successfully manufacture hybrid nanocomposites containing nanoparticles of titanium dioxide ($TiO_2$) and reduced graphene oxide (rGO) from tetrabutyl titanate (TBT) and graphene oxide (GO) powder using the hydrothermal method. For two hydrothermal treatment times (12h and 24h), various samples were created: $TiO_2$, rGO, and $TiO_2$/rGO nanocomposites thin films. Fourier transformer infrared (FTIR) spectra of the samples gave clear evidence for the reduction of GO and the engagement of Ti with reduced graphene by the formation of a Ti-O-C bond. The measurement of the energy band gap obtained by the photoluminescence spectrometer shows a decrease in the energy band gap for all samples after the hydrothermal reaction time increases, for the composite, the band gap decreases to 2.65 eV and 2.64 eV.

**Article Info.**

**Keywords:**
*$TiO_2$, rGO, Hydrothermal Method, Nanocomposite, Optical Properties.*

**Article history:**
*Received: Aug. 7, 2023*
*Revised: Oct. 22, 2023*
*Accepted: Oct. 30, 2023*
*Published: Mar.01,2024*

## 1. Introduction

Hybrid organic-inorganic materials have generated a great deal of attention lately because of their unique optical, electrical, and mechanical properties. These materials are composed of organic and inorganic components, resulting in a combination of properties not possible with either material alone. At the nanoscale and even the molecular scale, new methods for characterizing hybrid materials are being created [1-10]. The use of hybrid materials has increased in many significant fields, including sensors, electronics, optics, lightning, medicine, catalysis, energy storage, and energy conversion. The study of optical materials, which has numerous applications in fields such as bioimaging, screen design, optoelectronics, lighting, and energy, has seen great success with the development of hybrid materials. This is partly because creating extremely new optical systems at the macro or nanoscales, combining the mechanical or optical properties of inorganic materials with the distinctive optical responses of organic molecule species constitutes a revolutionary method [10-16]. The interfaces between organic and inorganic substances are crucial because optical processes are extremely sensitive to their surroundings in most systems [16-19]. Titanium dioxide ($TiO_2$) and reduced graphene oxide (rGO) nanocomposite is one example of a hybrid organic-inorganic material.

$TiO_2$ is a semiconducting material with remarkable physical and chemical properties. It is affordable, nontoxic, and has high chemical and mechanical stability [20, 21]. For all its favorable features, $TiO_2$ can be utilized in many different applications, including gas sensors, self-cleaning electrochromic devices, self-cleaning solar cells, photocatalysis applications, and many more. rGO is a derivative of graphene oxide (GO) obtained through the reduction of the oxygen-containing functional groups in GO. It possesses excellent electrical conductivity, mechanical strength, and flexibility, making it an attractive candidate for enhancing the electrical and optical

This work is licensed under a Creative Commons Attribution 4.0 International License.

properties of composites [22, 23]. The combination of $TiO_2$ and rGO is expected to produce a synergistic effect, resulting in superior optical properties and improved performance compared to individual materials [24]. The synthesis of $TiO_2$/rGO nanocomposite via the hydrothermal method offers a promising approach to achieve intimate interfacial interaction between $TiO_2$ and rGO. The prepared nanomaterials by the hydrothermal method under specific temperature and pressure conditions enable the synthesis of thin films with controlled morphology and high crystallinity [25, 26].

This study investigates the optical properties of (rGO/$TiO_2$) nanocomposite thin films synthesized by the drop casting method. The optical properties and characterization were done using the photoluminescence (PL) analysis and Fourier-transform infrared spectroscopy (FTIR). PL can provide an understanding of the electronic structure and emission behavior of the nanocomposite, while FTIR is capable of identifying functional groups and providing information about surface chemistry and bonding configurations.

## 2. Experimental Methods

### 2.1. Materials

Graphene oxide powder (GO) was obtained from nano-meter.ir, deionized water, 100% ethanol solution, acetic acid and tetrabutyl titanate (TBT) manufactured by Sigma Aldrich.

### 2.2. ($TiO_2$-rGO) Nanocomposites Synthesis

The $TiO_2$, and rGO were prepared using a simple method of two steps, In the first step, rGO and $TiO_2$ were separately prepared by dispersing 300 mg of GO powder (purchase from Nano-scale, Iran) in 2.5 mL of tetrabutyl titanate (TBT) (from Sigma Aldrich) in a solution containing 2.5 mL of water, 5 mL of ethanol, and 5 mL of acetic acid and stirring it magnetically for 10 min. The second step was the hydrothermal treatment of the two solutions in a 50ml Teflon-sealed autoclave at 180$^o$C for different times (12h and 24h). The autoclave was cooled to room temperature after hydrothermal treatment, washed multiple times with absolute ethanol and DI water, and dried in a vacuum drying oven at 70$^o$C for 10 hrs. The preparation of $TiO_2$/rGO nanocomposite was by mix the two sol-gel of $TiO_2$ and GO prepared in the first step and also putted into a 50 ml of Teflon-sealed autoclave and maintained at 180$^o$C for 12hrs and purified by washing as mentioned above. The prepared samples are labeled as in Table 1.

The ($TiO_2$-rGO) nanocomposites thin films samples were prepared by the drop casting process and dried at room temperature before being thermally treated at 60°C for 30 mins. The prepared samples are labeled as shown in Table 1.

***Table 1: Samples symbol.***

| Samples | Symbol |
|---|---|
| ($TiO_2$)-12h | T1 |
| ($TiO_2$)-24h | T2 |
| (rGO)-12h | R1 |
| (rGO)-24h | R2 |
| ($TiO_2$-rGO)-12h | C1 |
| ($TiO_2$-rGO)-24h | C2 |

## 3. Results and Discussion

### 3.1. FTIR

The FTIR spectra of the samples (T1, T2, R1, R2, C1, C2) obtained with an FTIR spectrometer (8400S, Shimadzu, Japan) are shown in Fig.1. All showed broad peaks in the range of 3700-2600 $cm^{-1}$, which is attributable to hydroxyl groups at various positions (O-H stretching of interacting hydroxyl groups, as well as molecular water's symmetric and asymmetric O-H stretching modes). The T1 and T2 samples are distinguished by a wide peak at 525 $cm^{-1}$ and 820 $cm^{-1}$, representing Ti–O–Ti band and Ti-O skeletal frequency, respectively [27-30]. For R1 and R2 samples, the characteristic peaks which indicate the reduction process of graphene oxide were at 1240 and 1060 $cm^{-1}$ assigned to the C–O–C (epoxy) and C–O (alkoxy) stretching vibrations, respectively, the peak at 1570 $cm^{-1}$ belongs to the C=O bands [31, 32]. For C1and C2 samples, the peaks observed below 1000 $cm^{-1}$ are broader and shifted to a higher wavenumber compared to the corresponding band in T1 and T2 samples. This band is presumably a combination of Ti-O-Ti vibration and Ti-O-C vibration modes resulting from the chemical interaction of $TiO_2$ with rGO. The presence of Ti-O-C bands suggests that, during the hydrothermal treatment, the oxygen-containing functional groups of GO interacted strongly with the surface hydroxyl groups of $TiO_2$ nanoparticles ensuring that the nanoparticles remained attached, even after chemical cleaning and ultrasonication, to eventually afford the chemically-bonded $TiO_2$/rGO nanocomposites, which verify the successful synthesis of the nanocomposites [33-35].

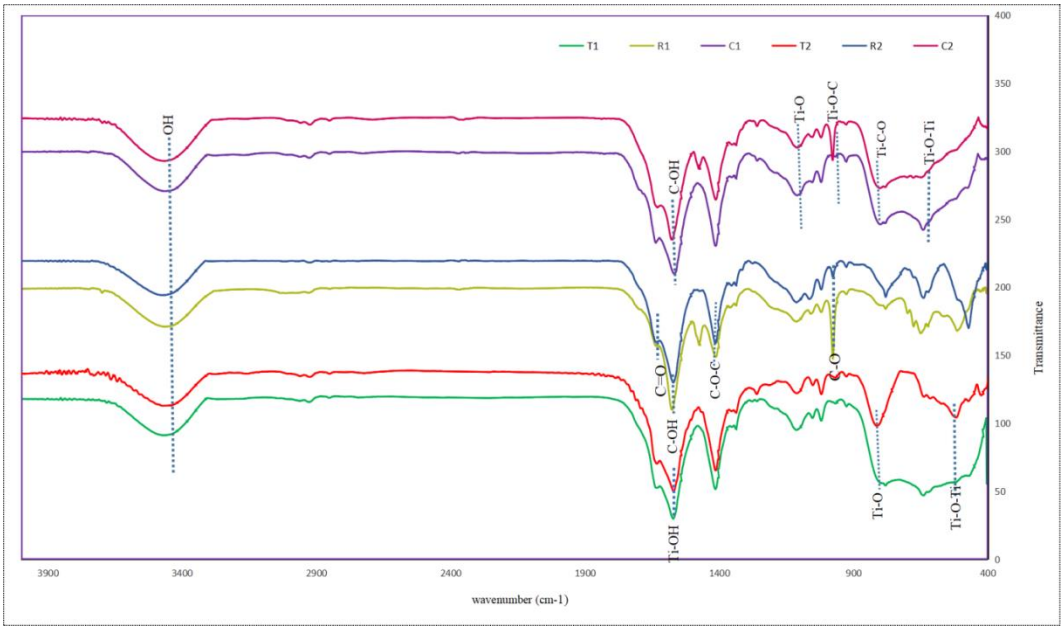


***Figure 1: FTIR spectra for $TiO_2$-rGO nanocomposites' for two hydrothermal reaction times (12–24 hrs).***

### 3.2. Photoluminescence (PL) Analysis

The PL measurement, using a photoluminescence spectrometer (Shimadzu, Japan), results of samples T1 and T2 are shown in Fig.2. Both samples exhibited similar behavior with strong peaks at wavelengths 378 and 380 nm, respectively, which correspond to the emission of bandgap transitions with light energies close to the anatase bandgap energy (387.5 nm) [36]. Exciton PL produces additional peaks at wavelengths of 398, 454, 470, 484, and 495 nm, which are mainly caused by surface oxygen vacancies and defects [37, 38]. Fig.3 shows that the R1 and R2 samples each have a single peak, at 464 nm for the R1 sample, and at 467 nm with decreased intensity

for the R2 sample. When exposed to light, the composite has a lower rate of electron and hole recombination than $TiO_2$ nanoparticles, as shown in Fig.4, where PL sensitivity of $TiO_2$-rGO (C1 and C2 samples) was noticeably lower than that of $TiO_2$ nanoparticles (T1 and T2 samples) [39, 40]. This phenomenon is ascribed to the fact that electrons are excited from the valence band to the conduction band and then transferred to rGO sheets due to its excellent electronic conductivity, preventing direct recombination of electrons and holes [41-43]. the other reason may be due to the quenching effect of rGO, that is, some of the generated photoluminescence is absorbed by rGO. The energy gaps of prepared samples are listed in Table 2.

***Table 2. the Energy gap of the prepared samples.***

| Samples | Energy gap(eV) |
|---|---|
| T1 | 3.28 |
| T2 | 3.26 |
| R1 | 2.67 |
| R2 | 2.65 |
| C1 | 2.65 |
| C2 | 2.64 |

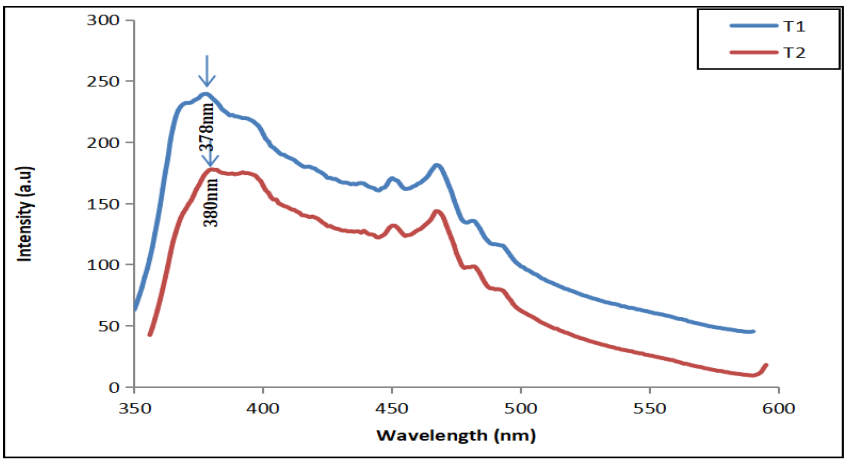


***Figure 2: T1 and T2 samples photoluminescence spectra.***

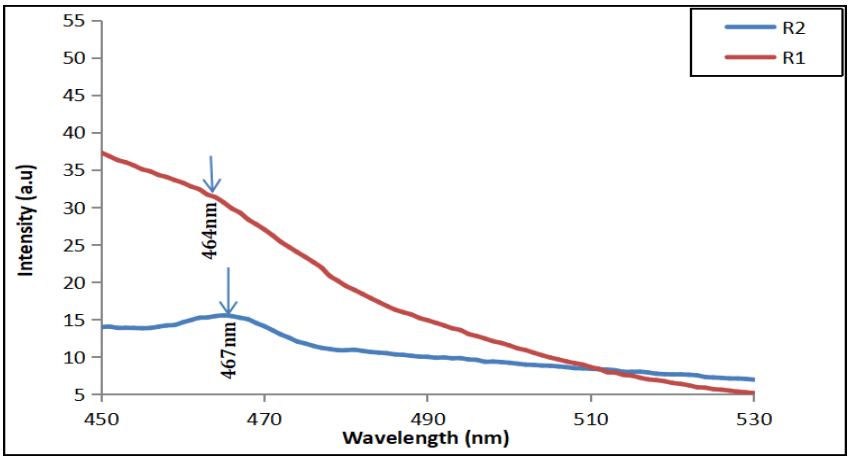


***Figure 3: R1 and R2 samples photoluminescence spectra.***

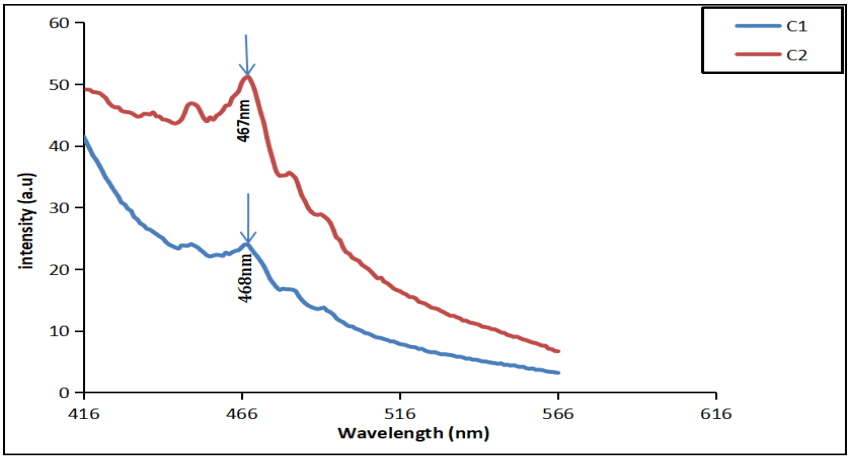


***Figure 4: C1 and C2 samples photoluminescence spectra .***

## 4. Conclusions

Without using any inorganic or organic reducing agents, $TiO_2$, rGO, $TiO_2$/rGO nanocomposite were successfully synthesized using the hydrothermal method. FTIR results confirmed the formation of rGO by indicating its functional groups as well as the formation of Ti–O–C bonds between rGO and $TiO_2$ verifying the formation of the nanocomposite. The photoluminescence measurements of the synthesized material showed a reduction in the energy gap of the nanocomposite after the incorporation of $TiO_2$ with rGO.

## Conflict of interest

Authors declare that they have no conflict of interest.

## References

1. I. Blanco, Appl. Sci. **10**, 5456 (2020).
2. J.-M. García-Martínez and E. P. Collar, Polymers **13**, 2390 (2021).
3. S. Singh, H. Chen, S. Shahrokhi, L. P. Wang, C.-H. Lin, L. Hu, X. Guan, A. Tricoli, Z. J. Xu, and T. Wu, ACS En. Lett. **5**, 1487 (2020).
4. J. Zhang, M. De Souza, C. Creighton, and R. J. Varley, Comp. Part A: Appl. Sci. Manufac. **133**, 105870 (2020).
5. M. Romero, D. Mombrú, F. Pignanelli, R. Faccio, and A. W. Mombrú, Front. Chem. **10**, 892013 (2022).
6. Y. Chujo, Curr. Opin. Sol. Stat. Mat. Sci. **1**, 806 (1996).
7. M. M. Adnan, A. R. Dalod, M. H. Balci, J. Glaum, and M.-A. Einarsrud, Polymers **10**, 1129 (2018).
8. J.-M. García-Martínez and E. P. Collar, Polymers **13**, 86 (2020).
9. D. Bin, W. Huo, Y. Yuan, J. Huang, Y. Liu, Y. Zhang, F. Dong, Y. Wang, and Y. Xia, Chem **6**, 968 (2020).
10. H. Eckert, M. Montagna, A. Dianat, R. Gutierrez, M. Bobeth, and G. Cuniberti, BMC Mat. **2**, 1 (2020).
11. B. R. Gomes, R. B. Figueira, S. P. Costa, M. M. M. Raposo, and C. J. Silva, Polymers **12**, 2671 (2020).
12. B. Valeur and M. N. Berberan-Santos, *Molecular fluorescence: principles and applications* (Weinheim, Germany, John Wiley & Sons, 2012).
13. Q. M. Al-Bataineh, A. A. Ahmad, A. M. Alsaad, and A. Telfah, Polymers **12**, 2954 (2020).
14. A. Köhler, J. S. Wilson, and R. H. Friend, Advan. Mat. **14**, 701 (2002).
15. C. Sanchez and F. Ribot, New J. Chem. **18**, 1007 (1994).

16. G. Kickelbick, *Hybrid Materials: Synthesis, Characterization, and Applications* (Weinheim, Wiley-VCH Verlag GmbH & Co. KGaA, 2006).
17. J. K. Pandey, A. P. Kumar, M. Misra, A. K. Mohanty, L. T. Drzal, and R. Palsingh, J,. Nanosci. Nanotech. **5**, 497 (2005).
18. R. S. Alnayli, H. Alkhazaali, and Z. Hakim, Journal of Physics: Conference Series (IOP Publishing, 2019). p. 012040.
19. H. M. Aziz, M. H. Al-Mamoori, and L. H. Aboud, Journal of Physics: Conference Series (IOP Publishing, 2021). p. 012206.
20. K. K. Ng and G. Zheng, Chem. Rev. **115**, 11012 (2015).
21. S. D. Al-Algawi, R. T. R. Rasheed, and Z. R. Rhoomi, Iraqi J. Sci. **58**, 1683 (2017).
22. H. A. Hessain and J. Hassan, Iraqi J. Sci. **61**, 1313 (2020).
23. X. Xiang, Y. Lu, and J. Chen, Acta Chim. Sin. **75**, 154 (2017).
24. B. Tang, H. Chen, H. Peng, Z. Wang, and W. Huang, Nanomaterials **8**, 105 (2018).
25. I. Ali and J.-O. Kim, Catalysts **8**, 43 (2018).
26. F. Nazeer, J. Long, Z. Yang, and C. Li, Nanotechnology **32**, 435701 (2021).
27. C. Cha, S. R. Shin, N. Annabi, M. R. Dokmeci, and A. Khademhosseini, ACS Nano **7**, 2891 (2013).
28. K. M. Al-Qahtani, M. H. Ali, and A. G. Al-Afify, J. Element. **25**, 315 (2020).
29. H. P. Mungse, S. Verma, N. Kumar, B. Sain, and O. P. Khatri, J. Mat. Chem. **22**, 5427 (2012).
30. N. Yang, J. Zhai, D. Wang, Y. Chen, and L. Jiang, ACS Nano **4**, 887 (2010).
31. N. Jantarasorn, O. Mekasuwandumrong, P. Kelly, and P. Praserthdam, IOP Conference Series: Materials Science and Engineering (IOP Publishing, 2019). p. 012017.
32. J.-G. Yu, H.-G. Yu, B. Cheng, X.-J. Zhao, J. C. Yu, and W.-K. Ho, J. Phys. Chem. B **107**, 13871 (2003).
33. G. a. S. Juárez, E. G. Barojas, E. Quiroga-González, E. Sánchez-Mora, and J. D. Santamaría-Juárez, Euro. J. Eng. Tech. Res. **4**, 165 (2019).
34. A. Daway Thamir, A. J Haider, and G. A Ali, Eng. Tech. J. **34**, 193 (2016).
35. R. A. Abd Ali, M. R. Al-Bahrani, and H. H. Waried, NeuroQuantology **20**, 5338 (2022).
36. Z. Ye, L. Zhao, A. Nikiforov, J.-M. Giraudon, Y. Chen, J. Wang, and X. Tu, Advan. Coll. Inter. Sci. **308**, 102755 (2022).
37. Y. Wang and N. Herron, J. Phys. Chem. **92**, 4988 (1988).
38. M. Rajabi and S. Shogh, J. Lumin. **157**, 235 (2015).
39. D. Xu, P. Wang, and B. Shen, Dig. J. Nanomat. Biostruct. **11**, 15 (2016).
40. J. S. Park, S. M. Cho, W.-J. Kim, J. Park, and P. J. Yoo, ACS Appl. Mat. Inter. **3**, 360 (2011).
41. K. Li, Y. Zhu, Y. Zhang, D. Zhang, J. Zhou, X. Li, and S. Ruan, Nanotechnology **30**, 295502 (2019).
42. F. Dai, S. Zhang, Q. Wang, H. Chen, C. Chen, G. Qian, and Y. Yu, Front. Chem. **9**, 753741 (2021).
43. Y. Yao, G. Li, S. Ciston, R. M. Lueptow, and K. A. Gray, Envir. Sci. Tech. **42**, 4952 (2008).

# دراسة بصرية لأغشية رقيقة من أكسيد الجرافين المختزل / ثاني أكسيد التيتانيوم النانوية المحضرة بالطريقة الحرارية المائية

**ليندا اسماعيل محي[1] واامير فيصل عبد الامير[1]**
*[1]قسم الفيزياء، كلية العلوم، جامعة بغداد، بغداد، العراق*

## الخلاصة

إن الحاجة المتزايدة للخصائص البصرية الفريدة في صناعة الأجهزة الإلكترونية دفعت العالم إلى مجال المواد الهجينة ومركباتها. في هذه الدراسة، تم استخدام تقنية فيزيائية بسيطة لتصنيع مركبات نانوية هجينة تحتوي على جسيمات متناهية الصغر من ثاني أكسيد التيتانيوم وأكسيد الجرافين المخفض من تيتانات رباعي *بوتيل* (TBT) ومسحوق أكسيد الجرافين GO بنجاح باستخدام الطريقة الحرارية المائية تم استخدام الطريقة الحرارية المائية لتصنيع مركبات نانوية هجينة تحتوي على جسيمات متناهية الصغر من ثاني أكسيد التيتانيوم وأكسيد الجرافين المختزل بنجاح. تم إنتاج عينات مختلفة عن طريق تغيير زمن التحضير الحراري المائي. وأطياف FTIR تعطي دليلًا واضحًا على اختزال أكسيد الجرافين وتفاعل Ti مع الجرافين من خلال تكوين رابطة Ti-O-C. تظهر فجوة الطاقة الضوئية التي تم الحصول عليها بواسطة مطياف اللمعان الضوئي انخفاضًا في فجوة الطاقة لجميع العينات بعد زيادة وقت التفاعل الحراري المائي، بالنسبة للمركب، تنخفض فجوة الطاقة إلى 2.64ev ,2.65ev.

**الكلمات المفتاحية:** $TiO_2$، rGO، الطريقة الحرارية المائية، مركب نانوي، خصائص بصريه.